arXiv:1203.3410v2 [nucl-th] 23 Mar 2012

A study of the anisotropy associated with dipole asymmetry in heavy ion collisions

Jiangyong Jia,[1, 2] Sooraj K. Radhakrishnan,[1] and Soumya Mohapatra[1]
[1]*Department of Chemistry, Stony Brook University, Stony Brook, NY 11794, USA*
[2]*Physics Department, Brookhaven National Laboratory, Upton, NY 11796, USA*

The anisotropy associated with the initial dipole asymmetry in heavy ion collisions is studied via the two-particle relative azimuthal azimuthal angle ($\Delta\phi = \phi^{\rm a} - \phi^{\rm b}$) correlations, within a multi-phase transport model. For a broad selection of centrality, transverse momenta ($p_{\rm T}^{\rm a,b}$) and pseudorapidity ($\eta^{\rm a,b}$), a fitting method is used to decompose the anisotropy into a rapidity-even component, characterized by the Fourier coefficient v_1, and a global momentum conservation component. The extracted v_1 values are negative for $p_{\rm T} \lesssim 0.7 - 0.9$ GeV, reach a maximum at 2-3 GeV, and decreases at higher $p_{\rm T}$. The v_1 values vary weakly with η and centrality, but increases with collision energy and parton cross-section. The extracted global momentum conservation component is found to depend on $\Delta\eta = \eta^{\rm a} - \eta^{\rm b}$ for $|\Delta\eta| < 3$.

PACS numbers: 25.75.-q

A large azimuthal anisotropy is observed for particle production in heavy ion collisions at the Relativistic Heavy Ion Collider (RHIC) and the Large Hadron Collider (LHC). This anisotropy is understood as the result of pressure-driven collective flow, which converts the spatial asymmetries of the initially created matter into transverse momentum ($p_{\rm T}$) space [1]. Such anisotropy can be expressed as Fourier series in azimuthal angle (ϕ):

$$\frac{dN}{d\phi} \propto 1 + 2\sum_{n=1}^{\infty} v_n(p_{\rm T}) \cos n(\phi - \Phi_n), \qquad (1)$$

where v_n and Φ_n represent the magnitude and direction of $n^{\rm th}$-order flow respectively. Asymmetries giving rise to non-zero v_n are associated with either an average shape (for $n = 2$) or shapes due to the spatial fluctuations of the participating nucleons [2–5]; the $n = 1$ term is known as dipole asymmetry. Due to the approximate boost invariance of the created matter, the v_n are expected to be even functions in rapidity (rapidity-even) [6, 7]. However, a small rapidity-odd v_n component, especially for $n = 1$, may arise from the "sideward" deflection of the created matter [8]. This rapidity-odd v_1 is expected to be very small for the rapidity range and the collision energies considered here [9–11], and is not considered in this paper.

The harmonics in Eq. 1 is also reflected in the two-particle correlation (2PC) in $\Delta\phi = \phi^{\rm a} - \phi^{\rm b}$:

$$\frac{dN_{\rm pairs}}{d\Delta\phi} \propto 1 + 2\sum_{n=1}^{\infty} v_{n,n}(p_{\rm T}^{\rm a}, p_{\rm T}^{\rm b}) \cos n\Delta\phi\ , \qquad (2)$$

with

$$v_{n,n}(p_{\rm T}^{\rm a}, p_{\rm T}^{\rm b}) = v_n(p_{\rm T}^{\rm a}) v_n(p_{\rm T}^{\rm b})\ . \qquad (3)$$

Recent studies at the LHC show that the latter factorization is valid for $n \geq 2$ at low $p_{\rm T}$ for particle pairs with a large rapidity gap [12, 13], but fails for $n = 1$ over the entire $p_{\rm T}$ range. This is understood to be due to global momentum conservation for a finite multiplicity system, which induces a negative dipole component in Eq. 3 [6, 14–17]:

$$v_{1,1}(p_{\rm T}^{\rm a}, p_{\rm T}^{\rm b}) \;=\; v_1(p_{\rm T}^{\rm a}) v_1(p_{\rm T}^{\rm b}) - c p_{\rm T}^{\rm a} p_{\rm T}^{\rm b} \qquad (4)$$

$$c \;=\; \frac{1}{KM\langle p_{\rm T}^2\rangle} \qquad (5)$$

where M is the total multiplicity in the event and K is the fraction of particles that are correlated via momentum conservation. A recent study by the ATLAS Collaboration [13] shows that $v_{1,1}$ can indeed be described by Eq. 4 over broad ranges of $p_{\rm T}^{\rm a,b}$. The v_1 values extracted via a two-component fit are negative for $p_{\rm T} \lesssim 1$ GeV, increase to a maximum at 4-5 GeV, and decrease at higher $p_{\rm T}$. A similar fitting method was previously applied by Retinskaya *et.al.* [18] to the ALICE 2PC data [19], although the data have less precision and may not be free of short range correlations due to smaller $\Delta\eta$ gap.

Many models based on viscous hydrodynamics or transport theory have been developed to describe the v_n and $v_{n,n}$ data [6, 20–27]. They show that sizable higher-oder flow ($n \geq 2$) can be generated by including fluctuations of the initial geometry. In some cases, reasonable agreement with the v_n data has been achieved. However, due to the complication associated with the global momentum conservation, most of these model attempts have avoided a prediction for v_1. Recently, Gardim *et.al* [6] performed the first calculation of the rapidity-even v_1 in a hydrodynamic code by directly cancelling the momentum conservation from $v_{1,1}$ by chosing appropriate weight for each particle (the cancellation is exact if the global conservation is linear in $p_{\rm T}$); a modified event plane (EP) method based on this cancellation procedure was also proposed [17]. Note that the systems that are related via momentum conservation could be smaller than the whole event (for example a dijet system) [28]. Therefore, the value of c (Eq. 5) may depend on other kinematic variables such as the $\Delta\eta$ of the particle pairs. Hence, it is

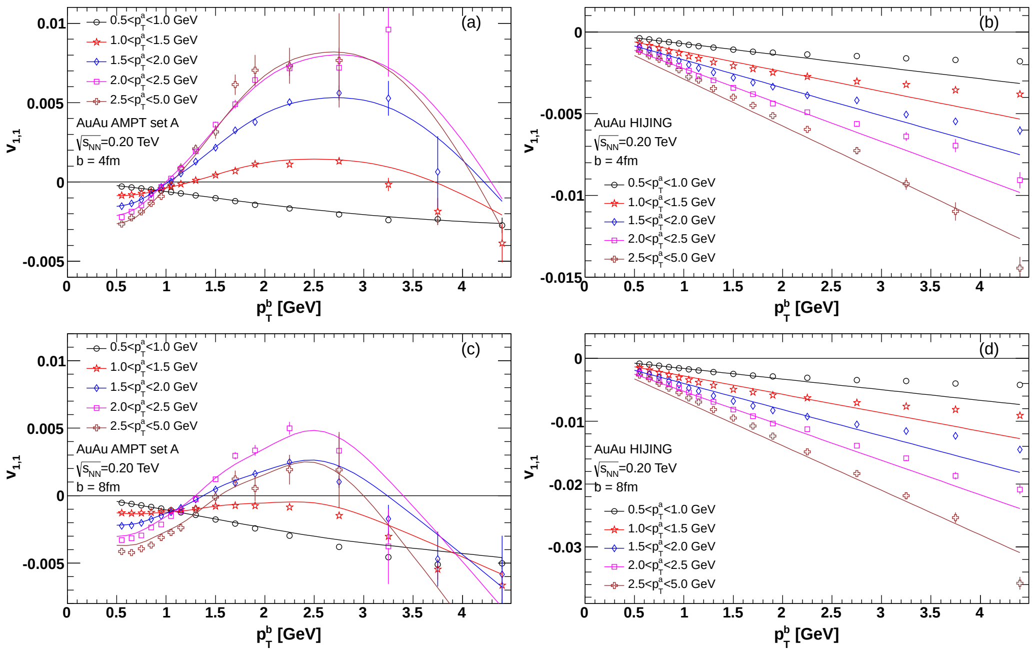

FIG. 1: (Color online) $v_{1,1}(p_{\rm T}^{\rm a}, p_{\rm T}^{\rm b})$ (symbols) from AMPT (left panels) and HIJING (right panels) for $b = 4$ fm (top panels) and $b = 8$ fm in AuAu collisions at $\sqrt{s_{NN}} = 0.2$ TeV. Lines in the left (right) panels are result of a global fit to Eq. 4 (a fit to pure momentum conservation component: $cp_{\rm T}^{\rm a}p_{\rm T}^{\rm b}$).

advantageous to determine c via the data driven method used by the ATLAS Collaboration.

In this work, we present a quantitative study of the rapidity-even v_1 using a generalization of the ATLAS fitting method within the AMPT (A Multi Phase Transport) model [29]. This study allows us to make quantitative predictions on how v_1 varies with $p_{\rm T}$, η, centrality, collision energy and partonic cross-section in a transport framework, as well as to compare with the ATLAS data.

The AMPT model has been successfully used to understand the higher-order v_n associated with initial asymmetries [20, 21, 23]. It combines the initial condition from HIJING [30] and final state interaction via a parton and hadron transport model. The initial condition from HIJING is seeded by a Glauber model for nucleon-nucleon scatterings, hence it contains the fluctuations which generate the event-by-event spatial asymmetries. The nucleon-nucleon scatterings provide both minijet partons for hard scattering and strings for soft coherent interactions; these strings are then converted into soft partons via a string melting scheme. The parton and hadron transport is responsible for transforming the initial asymmetries into the momentum anisotropy. The parton transport include only elastic scattering whose cross-sections are controlled by the values of the strong coupling constant (α_s) and the Debye screening mass (μ):

$$\frac{d\sigma}{dt} \approx \frac{9\pi\alpha_s^2}{2(t-\mu^2)^2}, \quad \sigma \approx 9\pi\alpha_s^2/(2\mu^2) \tag{6}$$

where t is the standard Mandelstam variable for four momentum transfer. Note that the total cross-section can be increased either with a larger α_s or a smaller value of μ. However changing α_s is more effective for momentum dissipation than changing μ, as decreasing μ includes only softer scattering (Eq. 6). Partons are recombined into hadrons at the freezeout, followed by a hadronic transport.

AMPT events are generated for two different α_s values for parton transport: set-A with $\alpha_s = 0.47$ and set-B with $\alpha_s = 0.33$ from [21] [31]. We vary the total cross-section from 1.5 mb to 10 mb by adjusting μ, separately for set-A and set-B. Varying α_s and μ allows us to study how v_1 depends on the strength of final state interactions. These studies are carried out at RHIC energy (Au+Au at $\sqrt{s_{NN}} = 0.2$ TeV) and/or LHC energy (Pb+Pb at $\sqrt{s_{NN}} = 2.76$ TeV) for the impact parameters $b = 4$ fm and $b = 8$ fm, corresponding to approximately 0-10% and 30-40% most central events, respectively.

We follow the procedure of extracting v_1 as documented in [13]. First, the correlation function for a given $p_{\rm T}^{\rm a}$, $p_{\rm T}^{\rm b}$ and $\Delta\eta$ range is constructed from all final state particles, and $v_{1,1}(p_{\rm T}^{\rm a}, p_{\rm T}^{\rm b}, \Delta\eta)$ values are calculated. Second, a least-square minimization of these $v_{1,1}$ values following Eq. 4 is used to obtain $v_1^{\rm Fit}(p_{\rm T})$ for a given $\Delta\eta$ range, where the $v_1^{\rm Fit}(p_{\rm T})$ function is defined by its values at 9 $p_{\rm T}$ points (0.5,0.7,0.9,1.1,1.5,2.0,3.0,3.8,4.6 GeV) via a cubic-spline interpolation procedure.

Figure 1 (a) and (c) show examples of such a study at RHIC energy, with the fit overlaid with the $v_{1,1}$ from AMPT for set-A with a 10mb partonic cross-section. A rapidity gap of 1.5 is imposed to suppress the short range correlations. The $v_{1,1}$ values for different $p_{\rm T}^{\rm a}$ selections cross each other and change sign as one increase $p_{\rm T}^{\rm a,b}$, a feature qualitatively similar to the ATLAS data.

Figure 1 (b) and (d) show the $v_{1,1}$ values obtained from HIJING, which has no final state interaction. They vary nearly linearly with $p_{\rm T}^{\rm a} \times p_{\rm T}^{\rm b}$, consistent with behavior expected for global momentum conservation. This sug-

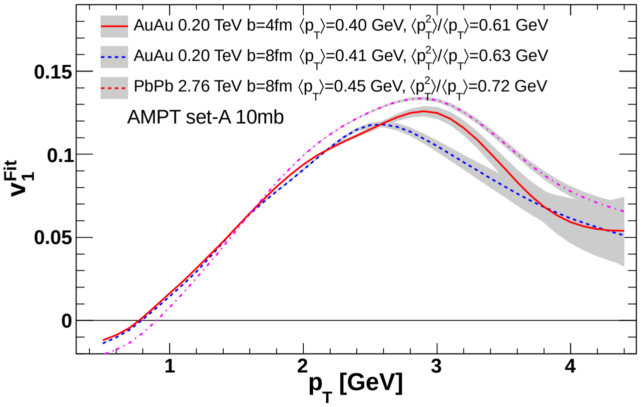

FIG. 2: (Color online) $v_1^{\rm Fit}$ vs $p_{\rm T}$ at RHIC energy and LHC.

gests that the complex dependence of the $v_{1,1}$ on $p_{\rm T}^{\rm a,b}$ in the left panels is a natural consequence of final state interactions.

Figure 2 shows $v_1^{\rm Fit}(p_{\rm T})$ extracted from the fit. The $v_1^{\rm Fit}$ function crosses zero at low $p_{\rm T}$, with the crossing point of $p_{\rm T,0} = 0.7 - 0.8$ GeV at RHIC energy and 0.9 GeV at LHC energy, respectively. Since the integral v_1 should be zero: $\langle p_{\rm T} v_1(p_{\rm T})\rangle = 0$, the change of $p_{\rm T,0}$ mainly reflects the change of the $\langle p_{\rm T}\rangle$ and $\langle p_{\rm T}^2\rangle$ (value shown in the legend). One can show that if $v_1(p_{\rm T})$ is a linear function of $p_{\rm T}$, the crossing point is $p_{\rm T,0} = \langle p_{\rm T}^2\rangle/\langle p_{\rm T}\rangle$. However, a change in the $\langle p_{\rm T}\rangle$ and $\langle p_{\rm T}^2\rangle$ should have little influence on the v_1 values at high $p_{\rm T}$; there the v_1 values are more sensitive to transport properties of the medium. The $v_1^{\rm Fit}(p_{\rm T})$ increases with $p_{\rm T}$ to a value ~ 0.1 at 2-3 GeV, and then decreases at higher $p_{\rm T}$. The $v_1^{\rm Fit}$ values for $b = 4$ fm and $b = 8$ fm are comparable, consistent with the lack of centrality dependence in the initial dipole asymmetry [4, 5]. The $v_1^{\rm Fit}$ value at LHC energy is larger, consistent with a stronger collective flow at LHC.

Figure 3 shows $v_1^{\rm Fit}(p_{\rm T})$ for set-A and set-B at different parton cross-sections tuned by changing μ. The magnitude of $v_1^{\rm Fit}(p_{\rm T})$ clearly grows with increasing cross-section. However the v_1 values are more sensitive to changes in α_s: a change of $\alpha_s = 0.47$ for set-A to 0.33 for set-B almost leads to a 60% increase of the peak value of v_1. Results for set-B with a 1.5 mb cross-section agree better with the ATLAS data at low $p_{\rm T}$. However both sets fail to describe the trend of the data for $p_{\rm T} > 3$ GeV. This reflects a limitation in the AMPT model for predicting the behavior of v_n at high $p_{\rm T}$: the jet quenching physics is important at high $p_{\rm T}$, but is not modelled correctly in AMPT. Similar studies for v_2 also found that the set-B 1.5 mb has the best agreement with the data for $p_{\rm T} < 2$ GeV [21].

The original fitting method of ATLAS can be generalized to measure the η dependence of v_1 in AMPT. We first perform the 2PC analysis in bins of $p_{\rm T}^{\rm a}, p_{\rm T}^{\rm b}, \eta^{\rm a}$, and $\eta^{\rm b}$. The resulting 4-D dataset $v_{1,1}(p_{\rm T}^{\rm a}, p_{\rm T}^{\rm b}, \eta^{\rm a}, \eta^{\rm b})$ is then parameterized by:

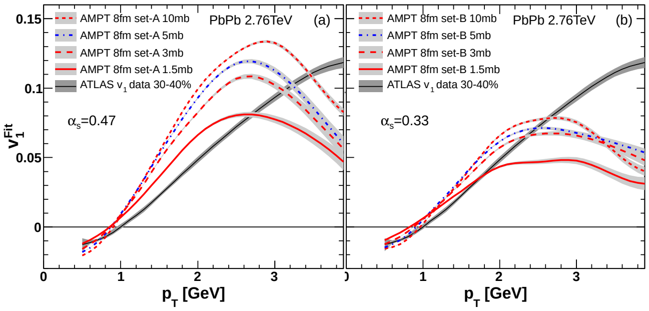

FIG. 3: (Color online) $v_1^{\rm Fit}$ vs $p_{\rm T}$ for set-A (left panels) and set-B (right panels) for impact parameter $b = 8$ fm, and compared with ATLAS Pb+Pb data.

$$
\begin{aligned}
v_{1,1}(p_{\rm T}^{\rm a}, p_{\rm T}^{\rm b}, \eta^{\rm a}, \eta^{\rm b}) \;=\; & v_1^{\rm Fit}(p_{\rm T}^{\rm a}, \eta^{\rm a}) v_1^{\rm Fit}(p_{\rm T}^{\rm b}, \eta^{\rm b}) \\
& - c(\eta^{\rm a}, \eta^{\rm b}) p_{\rm T}^{\rm a} p_{\rm T}^{\rm b} \;,
\end{aligned}
\tag{7}
$$

to directly obtain $v_1^{\rm Fit}(p_{\rm T}, \eta)$. A minimum $|\Delta\eta|$ separation for the pairs is imposed to suppress the short range non-flow correlations. Therefore the total number of $v_{1,1}$ data points used in the fit depends on this gap requirement and the binning in $p_{\rm T}$ and η.

In the default fit, both $v_1^{\rm Fit}$ and c functions are assumed to be symmetric in η i.e. $v_1^{\rm Fit}(\eta) = v_1^{\rm Fit}(-\eta)$ and $c(\eta^{\rm a}, \eta^{\rm b}) = c(-\eta^{\rm a}, -\eta^{\rm b})$. In addition, we also have $c(\eta^{\rm a}, \eta^{\rm b}) = c(\eta^{\rm b}, \eta^{\rm a})$. We divide the $|\eta| < 3$ into 12 equally spaced η bins and use the same 9 bins in $p_{\rm T}$ as for Fig 1 and 2. The fit uses a $12 \times 9 = 108$ mesh in $(\eta, p_{\rm T})$ space with a simple linear interpolation, which has 54 independent mesh nodes due to symmetry in η. This together with 24 parameters for c, gives a total of 78 fitting parameters. The quality of the fit is generally comparable to those shown in Fig. 1.

Figure 4 shows the η dependence of the v_1 obtained this way for two $p_{\rm T}$ bins. The error bands account for the statistical uncertainty as well as the variation of the fit result by changing the $|\Delta\eta|$ gap from 0.5 to 2.5. The $v_1^{\rm Fit}(\eta)$ generally shows a weak η-dependence at RHIC energy, especially in the more central collisions. At LHC energy, however, the $v_1^{\rm Fit}(\eta)$ shows a small dip at mid-rapidity. The physics behind this dip is currently under investigation, but probably is related to the stronger longitudinal flow at higher collision energy. Figure 5 shows the values of $c(\eta^{\rm a}, \eta^{\rm b})$ plotted as a function of $|\Delta\eta|$ for $b = 8$ fm at RHIC and LHC. They fall approximately on a common curve for $|\Delta\eta| > 2$, suggesting that c nearly depends only on $|\Delta\eta|$ for pairs with large rapidity separation. The values of c at large $|\Delta\eta|$ are not sensitive to the $|\Delta\eta|$ gap used in the global fit (compare the solid and open symbols), and they are three times larger than that calculated via Eq. 5 assuming $K = 1$ at LHC (right panel), but are comparable at RHIC (left panel).

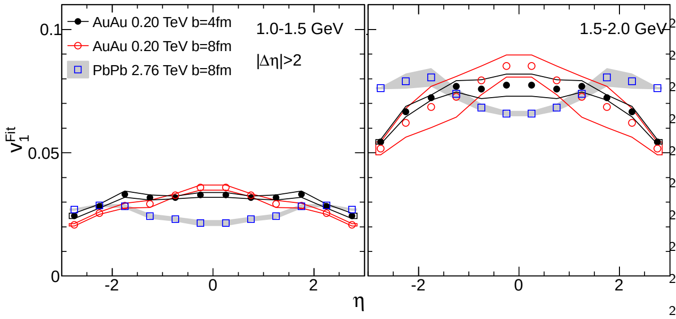

FIG. 4: v_1^{Fit} vs. η for two p_{T} ranges. They are determined from global fit of $v_{1,1}$ values for $|\Delta\eta| > 2$.

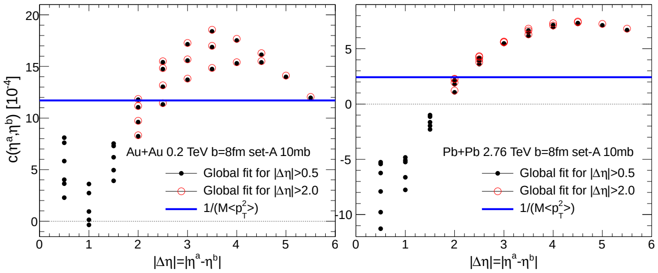

FIG. 5: $c(\eta^{\mathrm{a}}, \eta^{\mathrm{b}})$ vs. $|\eta^{\mathrm{a}} - \eta^{\mathrm{b}}|$ for $\Delta\eta > 0.5$ and $\Delta\eta > 2$ obtained from the Global fit. Data points at given $|\Delta\eta|$ value corresponds to different η^{a} and η^{b} combinations

In the original functional Eq. 4, parameter c is assumed to be a single number for each centrality class. Figure 5 clearly show that this is not the case in AMPT, and the global momentum conservation contribution changes with $|\Delta\eta|$. Some of this dependence is due to the influence of the short range correlations such as jet fragmentation and resonance decay, which tend to give a negative contribution to c at small $|\Delta\eta|$. However, the values of c still change with $|\Delta\eta|$ up to $|\Delta\eta| = 3$ then seem to flatten out at higher $|\Delta\eta|$, but at a level much bigger that predicted by Eq. 5. This may suggest that evaluating c with all particles in the event might be incorrect. In the modified EP method of Ref. [17], a p_{T} dependent weight $w = p_{\mathrm{T}} - \langle p_{\mathrm{T}}^2 \rangle / \langle p_{\mathrm{T}} \rangle$ is calculated for each particle used in the EP calculation. Note that if c depends on η of the two particles, $\langle p_{\mathrm{T}}^2 \rangle$ and $\langle p_{\mathrm{T}} \rangle$ need to be calculated in bins of η, instead of a single number calculated over the full η range of the EP. In other words, the weight is a function of p_{T} and η: $w(p_{\mathrm{T}}, \eta) = p_{\mathrm{T}} - \langle p_{\mathrm{T}}^2 \rangle(\eta) / \langle p_{\mathrm{T}} \rangle(\eta)$.

In summary, we study the v_1 associated with the initial dipole asymmetry in the AMPT Monte Carlo model using $v_{1,1} = \langle \cos\Delta\phi \rangle$ obtained from the two-particle correlation technique. A global fit of the $v_{1,1}$ using the procedure from the ATLAS Collaboration [13] allows the simultaneous extraction of $v_1(p_{\mathrm{T}})$ and the global momentum conservation component. The extracted v_1 function is negative at low p_{T}, and increases with p_{T} until 2-3 GeV, qualitatively agreeing with the behavior predicted by the hydrodynamic models. The v_1 function shows very little centrality dependence but increases with collision energy and parton cross-sections, suggesting that its magnitude increases with the strength of the final state interactions. By choosing the parameters in AMPT carefully, reasonable agreement with the ATLAS data can be achieved for $p_{\mathrm{T}} < 2$ GeV, but not at higher p_{T}. The fitting method is extended to directly extract the η dependence of v_1 and the global momentum conservation component (Eq. 7). The extracted v_1 shows a weak dependence on η. The coefficient of global momentum conservation component is found to depend on $\Delta\eta$ and differs from that given by Eq. 5. This extended method should allow the extraction of the $v_1(p_{\mathrm{T}}, \eta)$ and validation of the EP method (It requires detector acceptance to $p_{\mathrm{T}} = 0$, which is usually not satisfied in actual experiment).

We acknowledge valuable discussions with Matthew Luzum and Jean-Yves Ollitrault, in particular, the relation between the event plane method and two-particle correlation method. We thank Roy Lacey for a careful proofreading of the manuscript. This research is supported by NSF under award number PHY-1019387.

[1] J. Y. Ollitrault, Phys. Rev. D **46**, 229 (1992).
[2] B. Alver and G. Roland, Phys. Rev. C **81**, 054905 (2010) [Erratum-ibid. C **82**, 039903 (2010)].
[3] B. H. Alver, C. Gombeaud, M. Luzum, J. -Y. Ollitrault, Phys. Rev. C **82**, 034913 (2010).
[4] P. Staig and E. Shuryak, Phys. Rev. C **84**, 034908 (2011).
[5] D. Teaney and L. Yan, Phys. Rev. C **83**, 064904 (2011).
[6] F. G. Gardim, F. Grassi, Y. Hama, M. Luzum and J. -Y. Ollitrault, Phys. Rev. C **83**, 064901 (2011)
[7] P. Bozek, W. Broniowski and J. Moreira, Phys. Rev. C **83**, 034911 (2011)
[8] S. A. Voloshin, A. M. Poskanzer, R. Snellings, arXiv:0809.2949 [nucl-ex].
[9] PHOBOS Collaboration, Phys. Rev. Lett. **97**, 012301 (2006).
[10] STAR Collaboration, Phys. Rev. Lett. **101**, 252301 (2008).
[11] ALICE Collaboration, J. Phys. G **38**, 124167 (2011).
[12] CMS Collaboration, arXiv:1201.3158 [nucl-ex].
[13] ATLAS Collaboration, arXiv:1203.3087 [hep-ex].
[14] N. Borghini, P. M. Dinh, J. -Y. Ollitrault, Phys. Rev. C **62**, 034902 (2000).
[15] N. Borghini, P. M. Dinh, J. -Y. Ollitrault, A. M. Poskanzer, S. A. Voloshin, Phys. Rev. C **66**, 014901 (2002).
[16] N. Borghini, Phys. Rev. C **75**, 021904 (2007).
[17] M. Luzum and J. Y. Ollitrault, Phys. Rev. Lett. **106**, 102301 (2011).
[18] E. Retinskaya, M. Luzum and J. -Y. Ollitrault, arXiv:1203.0931 [nucl-th].
[19] ALICE Collaboration, Phys. Lett. B **708**, 249 (2012).
[20] J. Xu and C. M. Ko, Phys. Rev. C **84**, 044907 (2011)
[21] J. Xu and C. M. Ko, Phys. Rev. C **84**, 014903 (2011), Phys. Rev. C **83**, 034904 (2011)

[22] J. Xu and C. M. Ko, Phys. Rev. C **83**, 021903 (2011)

[23] G. -L. Ma and X. -N. Wang, Phys. Rev. Lett. **106**, 162301 (2011)

[24] B. Schenke, S. Jeon and C. Gale, Phys. Rev. C **85**, 024901 (2012)

[25] Z. Qiu and U. W. Heinz, Phys. Rev. C **84**, 024911 (2011).

[26] Z. Qiu, C. Shen and U. W. Heinz, Phys. Lett. B **707**, 151 (2012)

[27] J. Takahashi, B. M. Tavares, W. L. Qian, R. Andrade, F. Grassi, Y. Hama, T. Kodama and N. Xu, Phys. Rev. Lett. **103**, 242301 (2009)

[28] Z. Chajecki and M. Lisa, Phys. Rev. C **79**, 034908 (2009)

[29] Z. -W. Lin, C. M. Ko, B. -A. Li, B. Zhang and S. Pal, Phys. Rev. C **72**, 064901 (2005)

[30] M. Gyulassy, X. -N. Wang, Comput. Phys. Commun. **83**, 307 (1994).

[31] set-A and set-B also uses different parameterization of the Lund fragmentations in HIJING, which affect mainly the total multiplicity but not v_1.